

Measurement of the Branching Fraction for Inclusive Semileptonic B Meson Decays

B. Aubert,¹ D. Boutigny,¹ J.-M. Gaillard,¹ A. Hicheur,¹ Y. Karyotakis,¹ J. P. Lees,¹ P. Robbe,¹ V. Tisserand,¹
A. Zghiche,¹ A. Palano,² A. Pompili,² J. C. Chen,³ N. D. Qi,³ G. Rong,³ P. Wang,³ Y. S. Zhu,³ G. Eigen,⁴ I. Ofte,⁴
B. Stugu,⁴ G. S. Abrams,⁵ A. W. Borgland,⁵ A. B. Breon,⁵ D. N. Brown,⁵ J. Button-Shafer,⁵ R. N. Cahn,⁵
E. Charles,⁵ M. S. Gill,⁵ A. V. Gritsan,⁵ Y. Groysman,⁵ R. G. Jacobsen,⁵ R. W. Kadel,⁵ J. Kadyk,⁵ L. T. Kerth,⁵
Yu. G. Kolomensky,⁵ J. F. Kral,⁵ C. LeClerc,⁵ M. E. Levi,⁵ G. Lynch,⁵ L. M. Mir,⁵ P. J. Oddone,⁵
T. J. Orimoto,⁵ M. Pripstein,⁵ N. A. Roe,⁵ A. Romosan,⁵ M. T. Ronan,⁵ V. G. Shelkov,⁵ A. V. Telnov,⁵
W. A. Wenzel,⁵ T. J. Harrison,⁶ C. M. Hawkes,⁶ D. J. Knowles,⁶ S. W. O'Neale,⁶ R. C. Penny,⁶ A. T. Watson,⁶
N. K. Watson,⁶ T. Deppermann,⁷ K. Goetzen,⁷ H. Koch,⁷ B. Lewandowski,⁷ K. Peters,⁷ H. Schmuecker,⁷
M. Steinke,⁷ N. R. Barlow,⁸ W. Bhimji,⁸ J. T. Boyd,⁸ N. Chevalier,⁸ P. J. Clark,⁸ W. N. Cottingham,⁸ C. Mackay,⁸
F. F. Wilson,⁸ K. Abe,⁹ C. Hearty,⁹ T. S. Mattison,⁹ J. A. McKenna,⁹ D. Thiessen,⁹ S. Jolly,¹⁰ A. K. McKemey,¹⁰
V. E. Blinov,¹¹ A. D. Bukin,¹¹ A. R. Buzykaev,¹¹ V. B. Golubev,¹¹ V. N. Ivanchenko,¹¹ A. A. Korol,¹¹
E. A. Kravchenko,¹¹ A. P. Onuchin,¹¹ S. I. Serebnyakov,¹¹ Yu. I. Skovpen,¹¹ A. N. Yushkov,¹¹ D. Best,¹²
M. Chao,¹² D. Kirkby,¹² A. J. Lankford,¹² M. Mandelkern,¹² S. McMahon,¹² D. P. Stoker,¹² C. Buchanan,¹³
S. Chun,¹³ H. K. Hadavand,¹⁴ E. J. Hill,¹⁴ D. B. MacFarlane,¹⁴ H. Paar,¹⁴ S. Prell,¹⁴ Sh. Rahatlou,¹⁴ G. Raven,¹⁴
U. Schwanke,¹⁴ V. Sharma,¹⁴ J. W. Berryhill,¹⁵ C. Campagnari,¹⁵ B. Dahmes,¹⁵ P. A. Hart,¹⁵ N. Kuznetsova,¹⁵
S. L. Levy,¹⁵ O. Long,¹⁵ A. Lu,¹⁵ M. A. Mazur,¹⁵ J. D. Richman,¹⁵ W. Verkerke,¹⁵ J. Beringer,¹⁶ A. M. Eisner,¹⁶
M. Grothe,¹⁶ C. A. Heusch,¹⁶ W. S. Lockman,¹⁶ T. Pulliam,¹⁶ T. Schalk,¹⁶ R. E. Schmitz,¹⁶ B. A. Schumm,¹⁶
A. Seiden,¹⁶ M. Turri,¹⁶ W. Walkowiak,¹⁶ D. C. Williams,¹⁶ M. G. Wilson,¹⁶ E. Chen,¹⁷ G. P. Dubois-Felsmann,¹⁷
A. Dvoretzki,¹⁷ D. G. Hitlin,¹⁷ F. C. Porter,¹⁷ A. Ryd,¹⁷ A. Samuel,¹⁷ S. Yang,¹⁷ S. Jayatilleke,¹⁸ G. Mancinelli,¹⁸
B. T. Meadows,¹⁸ M. D. Sokoloff,¹⁸ T. Barillari,¹⁹ P. Bloom,¹⁹ W. T. Ford,¹⁹ U. Nauenberg,¹⁹ A. Olivas,¹⁹
P. Rankin,¹⁹ J. Roy,¹⁹ J. G. Smith,¹⁹ W. C. van Hoek,¹⁹ L. Zhang,¹⁹ J. L. Harton,²⁰ T. Hu,²⁰ M. Krishnamurthy,²⁰
A. Soffer,²⁰ W. H. Toki,²⁰ R. J. Wilson,²⁰ J. Zhang,²⁰ D. Altenburg,²¹ T. Brandt,²¹ J. Brose,²¹ T. Colberg,²¹
M. Dickopp,²¹ R. S. Dubitzky,²¹ A. Hauke,²¹ E. Maly,²¹ R. Müller-Pfefferkorn,²¹ S. Otto,²¹ K. R. Schubert,²¹
R. Schwierz,²¹ B. Spaan,²¹ L. Wilden,²¹ D. Bernard,²² G. R. Bonneaud,²² F. Brochard,²² J. Cohen-Tanugi,²²
S. Ferrag,²² S. T'Jampens,²² Ch. Thiebaut,²² G. Vasileiadis,²² M. Verderi,²² A. Anjomshoaa,²³ R. Bernet,²³
A. Khan,²³ D. Lavin,²³ F. Muheim,²³ S. Playfer,²³ J. E. Swain,²³ J. Tinslay,²³ M. Falbo,²⁴ C. Borean,²⁵ C. Bozzi,²⁵
L. Piemontese,²⁵ A. Sarti,²⁵ E. Treadwell,²⁶ F. Anulli,²⁷ * R. Baldini-Ferrolì,²⁷ A. Calcaterra,²⁷ R. de Sangro,²⁷
D. Falciai,²⁷ G. Finocchiaro,²⁷ P. Patteri,²⁷ I. M. Peruzzi,²⁷ * M. Piccolo,²⁷ A. Zallo,²⁷ S. Bagnasco,²⁸ A. Buzzo,²⁸
R. Contri,²⁸ G. Crosetti,²⁸ M. Lo Vetere,²⁸ M. Macri,²⁸ M. R. Monge,²⁸ S. Passaggio,²⁸ F. C. Pastore,²⁸
C. Patrignani,²⁸ E. Robutti,²⁸ A. Santroni,²⁸ S. Tosi,²⁸ S. Bailey,²⁹ M. Morii,²⁹ R. Bartoldus,³⁰ G. J. Grenier,³⁰
U. Mallik,³⁰ J. Cochran,³¹ H. B. Crawley,³¹ J. Lamsa,³¹ W. T. Meyer,³¹ E. I. Rosenberg,³¹ J. Yi,³¹ M. Davier,³²
G. Grosdidier,³² A. Höcker,³² H. M. Lacker,³² S. Laplace,³² F. Le Diberder,³² V. Lepeltier,³² A. M. Lutz,³²
T. C. Petersen,³² S. Plaszczynski,³² M. H. Schune,³² L. Tantot,³² S. Trincaz-Duvoid,³² G. Wormser,³²
R. M. Bionta,³³ V. Brigljević,³³ D. J. Lange,³³ K. van Bibber,³³ D. M. Wright,³³ A. J. Bevan,³⁴ J. R. Fry,³⁴
E. Gabathuler,³⁴ R. Gamet,³⁴ M. George,³⁴ M. Kay,³⁴ D. J. Payne,³⁴ R. J. Sloane,³⁴ C. Touramanis,³⁴
M. L. Aspinwall,³⁵ D. A. Bowerman,³⁵ P. D. Dauncey,³⁵ U. Egede,³⁵ I. Eschrich,³⁵ G. W. Morton,³⁵ J. A. Nash,³⁵
P. Sanders,³⁵ D. Smith,³⁵ G. P. Taylor,³⁵ J. J. Back,³⁶ G. Bellodi,³⁶ P. Dixon,³⁶ P. F. Harrison,³⁶ R. J. L. Potter,³⁶
H. W. Shorthouse,³⁶ P. Strother,³⁶ P. B. Vidal,³⁶ G. Cowan,³⁷ H. U. Flaecher,³⁷ S. George,³⁷ M. G. Green,³⁷
A. Kurup,³⁷ C. E. Marker,³⁷ T. R. McMahon,³⁷ S. Ricciardi,³⁷ F. Salvatore,³⁷ G. Vaitsas,³⁷ M. A. Winter,³⁷
D. Brown,³⁸ C. L. Davis,³⁸ J. Allison,³⁹ R. J. Barlow,³⁹ A. C. Forti,³⁹ F. Jackson,³⁹ G. D. Lafferty,³⁹ A. J. Lyon,³⁹
N. Savvas,³⁹ J. H. Weatherall,³⁹ J. C. Williams,³⁹ A. Farbin,⁴⁰ A. Jawahery,⁴⁰ V. Lillard,⁴⁰ D. A. Roberts,⁴⁰
J. R. Schieck,⁴⁰ G. Blaylock,⁴¹ C. Dallapiccola,⁴¹ K. T. Flood,⁴¹ S. S. Hertzbach,⁴¹ R. Kofler,⁴¹ V. B. Koptchev,⁴¹
T. B. Moore,⁴¹ H. Staengle,⁴¹ S. Willocq,⁴¹ B. Brau,⁴² R. Cowan,⁴² G. Sciolla,⁴² F. Taylor,⁴² R. K. Yamamoto,⁴²
M. Milek,⁴³ P. M. Patel,⁴³ F. Palombo,⁴⁴ J. M. Bauer,⁴⁵ L. Cremaldi,⁴⁵ V. Eschenburg,⁴⁵ R. Kroeger,⁴⁵ J. Reidy,⁴⁵

D. A. Sanders,⁴⁵ D. J. Summers,⁴⁵ C. Hast,⁴⁶ P. Taras,⁴⁶ H. Nicholson,⁴⁷ C. Cartaro,⁴⁸ N. Cavallo,⁴⁸ G. De Nardo,⁴⁸ F. Fabozzi,⁴⁸ C. Gatto,⁴⁸ L. Lista,⁴⁸ P. Paolucci,⁴⁸ D. Piccolo,⁴⁸ C. Sciacca,⁴⁸ J. M. LoSecco,⁴⁹ J. R. G. Alsmiller,⁵⁰ T. A. Gabriel,⁵⁰ J. Brau,⁵¹ R. Frey,⁵¹ M. Iwasaki,⁵¹ C. T. Potter,⁵¹ N. B. Sinev,⁵¹ D. Strom,⁵¹ E. Torrence,⁵¹ F. Colecchia,⁵² A. Dorigo,⁵² F. Galeazzi,⁵² M. Margoni,⁵² M. Morandin,⁵² M. Posocco,⁵² M. Rotondo,⁵² F. Simonetto,⁵² R. Stroili,⁵² C. Voci,⁵² M. Benayoun,⁵³ H. Briand,⁵³ J. Chauveau,⁵³ P. David,⁵³ Ch. de la Vaissière,⁵³ L. Del Buono,⁵³ O. Hamon,⁵³ Ph. Leruste,⁵³ J. Ocariz,⁵³ M. Pivk,⁵³ L. Roos,⁵³ J. Stark,⁵³ P. F. Manfredi,⁵⁴ V. Re,⁵⁴ V. Speziali,⁵⁴ L. Gladney,⁵⁵ Q. H. Guo,⁵⁵ J. Panetta,⁵⁵ C. Angelini,⁵⁶ G. Batignani,⁵⁶ S. Bettarini,⁵⁶ M. Bondioli,⁵⁶ F. Bucci,⁵⁶ G. Calderini,⁵⁶ E. Campagna,⁵⁶ M. Carpinelli,⁵⁶ F. Forti,⁵⁶ M. A. Giorgi,⁵⁶ A. Lusiani,⁵⁶ G. Marchiori,⁵⁶ F. Martinez-Vidal,⁵⁶ M. Morganti,⁵⁶ N. Neri,⁵⁶ E. Paoloni,⁵⁶ M. Rama,⁵⁶ G. Rizzo,⁵⁶ F. Sandrelli,⁵⁶ G. Triggiani,⁵⁶ J. Walsh,⁵⁶ M. Haire,⁵⁷ D. Judd,⁵⁷ K. Paick,⁵⁷ L. Turnbull,⁵⁷ D. E. Wagoner,⁵⁷ J. Albert,⁵⁸ N. Danielson,⁵⁸ P. Elmer,⁵⁸ C. Lu,⁵⁸ V. Miftakov,⁵⁸ J. Olsen,⁵⁸ S. F. Schaffner,⁵⁸ A. J. S. Smith,⁵⁸ A. Tumanov,⁵⁸ E. W. Varnes,⁵⁸ F. Bellini,⁵⁹ G. Cavoto,^{58,59} D. del Re,⁵⁹ R. Faccini,^{14,59} F. Ferrarotto,⁵⁹ F. Ferroni,⁵⁹ E. Leonardi,⁵⁹ M. A. Mazzoni,⁵⁹ S. Morganti,⁵⁹ G. Piredda,⁵⁹ F. Safai Tehrani,⁵⁹ M. Serra,⁵⁹ C. Voena,⁵⁹ S. Christ,⁶⁰ G. Wagner,⁶⁰ R. Waldi,⁶⁰ T. Adye,⁶¹ N. De Groot,⁶¹ B. Franek,⁶¹ N. I. Geddes,⁶¹ G. P. Gopal,⁶¹ S. M. Xella,⁶¹ R. Aleksan,⁶² S. Emery,⁶² A. Gaidot,⁶² P.-F. Giraud,⁶² G. Hamel de Monchenault,⁶² W. Kozanecki,⁶² M. Langer,⁶² G. W. London,⁶² B. Mayer,⁶² G. Schott,⁶² B. Serfass,⁶² G. Vasseur,⁶² Ch. Yeche,⁶² M. Zito,⁶² M. V. Purohit,⁶³ A. W. Weidemann,⁶³ F. X. Yumiceva,⁶³ I. Adam,⁶⁴ D. Aston,⁶⁴ N. Berger,⁶⁴ A. M. Boyarski,⁶⁴ M. R. Convery,⁶⁴ D. P. Coupal,⁶⁴ D. Dong,⁶⁴ J. Dorfan,⁶⁴ W. Dunwoodie,⁶⁴ R. C. Field,⁶⁴ T. Glanzman,⁶⁴ S. J. Gowdy,⁶⁴ E. Grauges,⁶⁴ T. Haas,⁶⁴ T. Hadig,⁶⁴ V. Halyo,⁶⁴ T. Himel,⁶⁴ T. Hryn'ova,⁶⁴ M. E. Huffer,⁶⁴ W. R. Innes,⁶⁴ C. P. Jessop,⁶⁴ M. H. Kelsey,⁶⁴ P. Kim,⁶⁴ M. L. Kocian,⁶⁴ U. Langenegger,⁶⁴ D. W. G. S. Leith,⁶⁴ S. Luitz,⁶⁴ V. Luth,⁶⁴ H. L. Lynch,⁶⁴ H. Marsiske,⁶⁴ S. Menke,⁶⁴ R. Messner,⁶⁴ D. R. Muller,⁶⁴ C. P. O'Grady,⁶⁴ V. E. Ozcan,⁶⁴ A. Perazzo,⁶⁴ M. Perl,⁶⁴ S. Petrak,⁶⁴ H. Quinn,⁶⁴ B. N. Ratcliff,⁶⁴ S. H. Robertson,⁶⁴ A. Roodman,⁶⁴ A. A. Salnikov,⁶⁴ T. Schietinger,⁶⁴ R. H. Schindler,⁶⁴ J. Schwiening,⁶⁴ G. Simi,⁶⁴ A. Snyder,⁶⁴ A. Soha,⁶⁴ S. M. Spanier,⁶⁴ J. Stelzer,⁶⁴ D. Su,⁶⁴ M. K. Sullivan,⁶⁴ H. A. Tanaka,⁶⁴ J. Va'vra,⁶⁴ S. R. Wagner,⁶⁴ M. Weaver,⁶⁴ A. J. R. Weinstein,⁶⁴ W. J. Wisniewski,⁶⁴ D. H. Wright,⁶⁴ C. C. Young,⁶⁴ P. R. Burchat,⁶⁵ C. H. Cheng,⁶⁵ T. I. Meyer,⁶⁵ C. Roat,⁶⁵ R. Henderson,⁶⁶ W. Bugg,⁶⁷ H. Cohn,⁶⁷ J. M. Izen,⁶⁸ I. Kitayama,⁶⁸ X. C. Lou,⁶⁸ F. Bianchi,⁶⁹ M. Bona,⁶⁹ D. Gamba,⁶⁹ L. Bosisio,⁷⁰ G. Della Ricca,⁷⁰ S. Dittongo,⁷⁰ L. Lancieri,⁷⁰ P. Poropat,⁷⁰ L. Vitale,⁷⁰ G. Vuagnin,⁷⁰ R. S. Panvini,⁷¹ Sw. Banerjee,⁷² C. M. Brown,⁷² D. Fortin,⁷² P. D. Jackson,⁷² R. Kowalewski,⁷² J. M. Roney,⁷² H. R. Band,⁷³ S. Dasu,⁷³ M. Datta,⁷³ A. M. Eichenbaum,⁷³ H. Hu,⁷³ J. R. Johnson,⁷³ R. Liu,⁷³ F. Di Lodovico,⁷³ A. Mohapatra,⁷³ Y. Pan,⁷³ R. Prepost,⁷³ I. J. Scott,⁷³ S. J. Sekula,⁷³ J. H. von Wimmersperg-Toeller,⁷³ J. Wu,⁷³ S. L. Wu,⁷³ Z. Yu,⁷³ and H. Neal⁷⁴

(The BABAR Collaboration)

¹Laboratoire de Physique des Particules, F-74941 Annecy-le-Vieux, France

²Università di Bari, Dipartimento di Fisica and INFN, I-70126 Bari, Italy

³Institute of High Energy Physics, Beijing 100039, China

⁴University of Bergen, Inst. of Physics, N-5007 Bergen, Norway

⁵Lawrence Berkeley National Laboratory and University of California, Berkeley, CA 94720, USA

⁶University of Birmingham, Birmingham, B15 2TT, United Kingdom

⁷Ruhr Universität Bochum, Institut für Experimentalphysik 1, D-44780 Bochum, Germany

⁸University of Bristol, Bristol BS8 1TL, United Kingdom

⁹University of British Columbia, Vancouver, BC, Canada V6T 1Z1

¹⁰Brunel University, Uxbridge, Middlesex UB8 3PH, United Kingdom

¹¹Budker Institute of Nuclear Physics, Novosibirsk 630090, Russia

¹²University of California at Irvine, Irvine, CA 92697, USA

¹³University of California at Los Angeles, Los Angeles, CA 90024, USA

¹⁴University of California at San Diego, La Jolla, CA 92093, USA

¹⁵University of California at Santa Barbara, Santa Barbara, CA 93106, USA

¹⁶University of California at Santa Cruz, Institute for Particle Physics, Santa Cruz, CA 95064, USA

¹⁷California Institute of Technology, Pasadena, CA 91125, USA

¹⁸University of Cincinnati, Cincinnati, OH 45221, USA

¹⁹University of Colorado, Boulder, CO 80309, USA

²⁰Colorado State University, Fort Collins, CO 80523, USA

²¹Technische Universität Dresden, Institut für Kern- und Teilchenphysik, D-01062 Dresden, Germany

²²Ecole Polytechnique, LLR, F-91128 Palaiseau, France

- ²³University of Edinburgh, Edinburgh EH9 3JZ, United Kingdom
²⁴Elon University, Elon University, NC 27244-2010, USA
²⁵Università di Ferrara, Dipartimento di Fisica and INFN, I-44100 Ferrara, Italy
²⁶Florida A&M University, Tallahassee, FL 32307, USA
²⁷Laboratori Nazionali di Frascati dell'INFN, I-00044 Frascati, Italy
²⁸Università di Genova, Dipartimento di Fisica and INFN, I-16146 Genova, Italy
²⁹Harvard University, Cambridge, MA 02138, USA
³⁰University of Iowa, Iowa City, IA 52242, USA
³¹Iowa State University, Ames, IA 50011-3160, USA
³²Laboratoire de l'Accélérateur Linéaire, F-91898 Orsay, France
³³Lawrence Livermore National Laboratory, Livermore, CA 94550, USA
³⁴University of Liverpool, Liverpool L69 3BX, United Kingdom
³⁵University of London, Imperial College, London, SW7 2BW, United Kingdom
³⁶Queen Mary, University of London, E1 4NS, United Kingdom
³⁷University of London, Royal Holloway and Bedford New College, Egham, Surrey TW20 0EX, United Kingdom
³⁸University of Louisville, Louisville, KY 40292, USA
³⁹University of Manchester, Manchester M13 9PL, United Kingdom
⁴⁰University of Maryland, College Park, MD 20742, USA
⁴¹University of Massachusetts, Amherst, MA 01003, USA
⁴²Massachusetts Institute of Technology, Laboratory for Nuclear Science, Cambridge, MA 02139, USA
⁴³McGill University, Montréal, QC, Canada H3A 2T8
⁴⁴Università di Milano, Dipartimento di Fisica and INFN, I-20133 Milano, Italy
⁴⁵University of Mississippi, University, MS 38677, USA
⁴⁶Université de Montréal, Laboratoire René J. A. Lévesque, Montréal, QC, Canada H3C 3J7
⁴⁷Mount Holyoke College, South Hadley, MA 01075, USA
⁴⁸Università di Napoli Federico II, Dipartimento di Scienze Fisiche and INFN, I-80126, Napoli, Italy
⁴⁹University of Notre Dame, Notre Dame, IN 46556, USA
⁵⁰Oak Ridge National Laboratory, Oak Ridge, TN 37831, USA
⁵¹University of Oregon, Eugene, OR 97403, USA
⁵²Università di Padova, Dipartimento di Fisica and INFN, I-35131 Padova, Italy
⁵³Universités Paris VI et VII, Lab de Physique Nucléaire H. E., F-75252 Paris, France
⁵⁴Università di Pavia, Dipartimento di Elettronica and INFN, I-27100 Pavia, Italy
⁵⁵University of Pennsylvania, Philadelphia, PA 19104, USA
⁵⁶Università di Pisa, Scuola Normale Superiore and INFN, I-56010 Pisa, Italy
⁵⁷Prairie View A&M University, Prairie View, TX 77446, USA
⁵⁸Princeton University, Princeton, NJ 08544, USA
⁵⁹Università di Roma La Sapienza, Dipartimento di Fisica and INFN, I-00185 Roma, Italy
⁶⁰Universität Rostock, D-18051 Rostock, Germany
⁶¹Rutherford Appleton Laboratory, Chilton, Didcot, Oxon, OX11 0QX, United Kingdom
⁶²DAPNIA, Commissariat à l'Energie Atomique/Saclay, F-91191 Gif-sur-Yvette, France
⁶³University of South Carolina, Columbia, SC 29208, USA
⁶⁴Stanford Linear Accelerator Center, Stanford, CA 94309, USA
⁶⁵Stanford University, Stanford, CA 94305-4060, USA
⁶⁶TRIUMF, Vancouver, BC, Canada V6T 2A3
⁶⁷University of Tennessee, Knoxville, TN 37996, USA
⁶⁸University of Texas at Dallas, Richardson, TX 75083, USA
⁶⁹Università di Torino, Dipartimento di Fisica Sperimentale and INFN, I-10125 Torino, Italy
⁷⁰Università di Trieste, Dipartimento di Fisica and INFN, I-34127 Trieste, Italy
⁷¹Vanderbilt University, Nashville, TN 37235, USA
⁷²University of Victoria, Victoria, BC, Canada V8W 3P6
⁷³University of Wisconsin, Madison, WI 53706, USA
⁷⁴Yale University, New Haven, CT 06511, USA

(Dated: August 13, 2002)

A largely model-independent measurement of the inclusive electron momentum spectrum and branching fraction for semileptonic decays of B mesons is presented based on data recorded at the $\Upsilon(4S)$ resonance with the BABAR detector. Backgrounds from secondary charm decays are separated from prompt B decays using charge and angular correlations between the electron from one B meson and a high momentum electron tag from the second B meson. The resulting branching fraction is $\mathcal{B}(B \rightarrow Xe\nu) = (10.87 \pm 0.18(\text{stat}) \pm 0.30(\text{syst}))\%$. Based on this measurement we determine the CKM matrix element $|V_{cb}|$.

Measurements of semileptonic B meson decays are a good way to determine the CKM matrix elements $|V_{cb}|$ and $|V_{ub}|$, two of the parameters of the Standard Model. For $|V_{cb}|$, analyses of exclusive and inclusive decays have resulted in comparable precision. While most measured values of $\mathcal{B}(B \rightarrow X e \nu)$ are below 11% [1], theoretical calculations including perturbative QCD contributions predict values of 12% or above [2].

The measurement presented here employs the method introduced by ARGUS [3] and later used by CLEO [4], in which $B\bar{B}$ events are tagged by the presence of a high momentum lepton. As a tag, we choose electrons with momentum p^* in the interval 1.4 to 2.3 GeV/ c , where p^* is measured in the center-of-mass frame. A second electron in the event is taken as the signal lepton for which we require $p^* > 0.6$ GeV/ c , to avoid large backgrounds at lower momenta. Signal electrons are mostly from primary B decays if they are accompanied by a tag electron of opposite charge (unlike-sign). Those with a tag of the same charge (like-sign) originate predominantly from secondary decays of charm particles produced in the decay of the other B meson. Inversion of this charge correlation due to $B^0\bar{B}^0$ mixing is treated explicitly, and unlike-sign pairs with both electrons originating from the same B meson are isolated kinematically. With a small model-dependence on the estimated fraction of primary electrons below $p^* = 0.6$ GeV/ c , we infer the semileptonic B branching fraction from the background corrected ratio of unlike-sign electron pairs to tag electrons.

This measurement is based on data recorded in the year 2000 with the BABAR detector [5] at the PEP-II energy asymmetric e^+e^- storage ring [6] at SLAC. The detector consists of a five-layer silicon vertex tracker (SVT), a 40-layer drift chamber (DCH), a detector of internally-reflected Cherenkov light (DIRC), and an electromagnetic calorimeter (EMC) all embedded in a solenoidal magnetic field of 1.5 T and surrounded by an instrumented flux return (IFR). To ensure the high quality of the data, we have selected the largest contiguous block of events with identical and stable detector conditions in the year 2000, corresponding to an integrated luminosity of 4.1 fb^{-1} collected at the $\Upsilon(4S)$ resonance, and 0.97 fb^{-1} recorded about 40 MeV below the $\Upsilon(4S)$ peak (off-resonance).

Multihadron events are selected by requiring a charged track multiplicity of $N_{\text{ch}} > 4$, or $N_{\text{ch}} = 4$ plus at least 2 neutral energy deposits above 80 MeV in the EMC. Track pairs from converted photons are not included in N_{ch} , but count as one neutral particle. For further suppression of non- $B\bar{B}$ events, we require $R_2 < 0.6$, where R_2 is the ratio of Fox-Wolfram moments H_2/H_0 [7].

The electron momentum measurement and identification are critical for this analysis. For electron candidates we require hits in at least 12 DCH layers, and a polar angle θ within the EMC acceptance, i.e. $-0.72 < \cos \theta < 0.92$. To reduce the contamination from photon conversions and beam-gas background we require the track impact parameters in the plane perpendicular to the beams and along the detector axis to be less than 0.25 cm and 3.0 cm, respectively.

The track finding efficiency ϵ_{trk} is determined from data as a function of charged multiplicity, transverse momentum, polar and azimuthal angle. For signal electrons with $p^* > 0.6$ GeV/ c , the average efficiency is $(97.1 \pm 1.1)\%$.

Electron identification is based on the ratio of the energy in the EMC and the track momentum, E_{EMC}/p , the shower shape in the EMC, the specific energy loss dE/dx in the DCH, and the number of Cherenkov photons and the Cherenkov angle measured in the DIRC. Muons are eliminated on the basis of dE/dx and E_{EMC}/p . Taking into account the correlations between deposited energy and shape in hadronic showers, we combine probability density functions derived from data samples for each discriminating variable to construct the likelihood function $L(\xi)$, $\xi \in \{e, \pi, K, p\}$. A track is identified as an electron if

$$\frac{L(e)}{L(e) + 5 L(\pi) + L(K) + 0.1 L(p)} > 0.95 .$$

The weights roughly reflect the relative abundances, their exact values not being crucial for electron identification.

We measure the electron identification efficiency as a function of p^* and center-of-mass polar angle θ^* using radiative Bhabha events. For momenta $p^* > 0.6$ GeV/ c , the average efficiency is 92% (see Figure 1a). However, Monte Carlo simulations indicate that relative to radiative Bhabha events, the identification efficiency in $B\bar{B}$ events is reduced between $(4 \pm 2)\%$ at low momenta ($p^* < 1$ GeV/ c) and $(2 \pm 1)\%$ above $p^* = 1.6$ GeV/ c . We correct the measured efficiency for this momentum-dependent difference.

The misidentification rates for pions, kaons, and protons are extracted from control samples selected from data. Figure 1b shows the misidentification probabilities η_h per hadronic track, where the relative abundance of pions, kaons, and protons is taken from $B\bar{B}$ Monte Carlo simulation. The DCH and DIRC contribute significantly at low momenta, while the performance of the EMC increases with p^* . This leads to a minimum of 0.05% for η_h at $1 < p^* < 1.3$ GeV/ c . The relative systematic error is estimated to be 15% from the purities of the control samples and the uncertainties in the relative abundances.

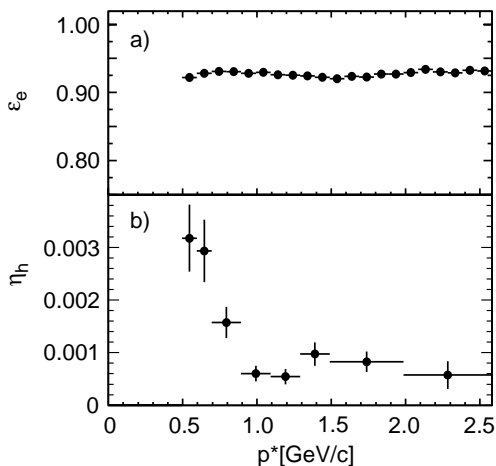


FIG. 1: Electron identification efficiency ϵ_e as obtained from radiative Bhabha events (a) and hadron misidentification rate η_h (b) as a function of p^* .

The branching fraction analysis makes use of three samples: (1) the tag electrons, (2) unlike-sign and (3) like-sign pairs of a tag and a signal electron candidate. Misidentified hadrons and electrons from non- $B\bar{B}$ (continuum) events, photon conversions, $\pi^0, \eta \rightarrow \gamma e^+ e^-$ (“Dalitz”) and $J/\psi, \psi(2S) \rightarrow e^+ e^-$ decays contribute to the background in all three samples. The unlike-sign sample also contains pairs of primary and secondary electrons from the same B meson decay. Further contaminations to the like- and unlike-sign samples arise from decays of τ leptons and charmed mesons produced in $b \rightarrow c\bar{c}s$ decays. Apart from the correction for unlike-sign electron pairs from the same B , which is performed in bins of p^* only, all background corrections are performed in bins of p^* and polar angle θ^* .

The continuum background is subtracted from all three samples. It is obtained by normalizing the observed off-resonance spectra by the ratio of on- to off-resonance integrated luminosities. The relative systematic error in this ratio is estimated to be 0.5%, attributed to variations in the detector performance over time. The continuum momenta are scaled by the ratio $\sqrt{s_{on}}/\sqrt{s_{off}}$ to compensate for the 0.4% lower center-of-mass energy.

Electrons from photon conversions and Dalitz decays are identified by pairing them with any oppositely charged track with transverse momentum $p_t > 0.1$ GeV/c. We distinguish the two sources of pairs by the distance R_{pair} of the pair vertex from the detector axis. Photon conversions are identified by requiring $R_{pair} > 1.6$ cm, a pair invariant mass $M_{ee} < 100$ MeV/c², and the transverse and longitudinal distances between the two tracks at the point of closest approach $\Delta_{xy} < 0.3$ cm and $\Delta_z < 1.0$ cm. For Dalitz pairs, we require $R_{pair} < 1.6$ cm,

$M_{ee} < 200$ MeV/c², $\Delta_{xy} < 0.2$ cm and $\Delta_z < 1.0$ cm. The momentum- and polar angle-dependent pair finding efficiency, which is obtained from a full detector simulation, is low since, in most cases, the momentum of the second track is too small to produce a track in the DCH. It varies between 30% and 40% for photon conversions and between 20% and 30% for Dalitz pairs. From a detailed comparison between data and simulation, including the energy spectra of the pairs, the relative systematic uncertainties are estimated to be 13% and 19% for the conversion and Dalitz background rates, respectively.

In the unlike-sign sample, electrons from primary and charm decays of the same B tend to be produced in opposite directions. Defining \hat{p}_e^* as the center of the signal electron momentum bin, this background is reduced by a factor of 24 by imposing the condition

$$\cos \alpha > 1.0 - \hat{p}_e^* / (\text{GeV}/c) \quad \text{and} \quad \cos \alpha > -0.2 \quad (1)$$

on the opening angle α of $e^+ e^-$ pairs, measured in the $\Upsilon(4S)$ frame. Since B mesons are nearly at rest in this frame, there is no angular correlation between two electrons from different B mesons, and the loss in signal efficiency can be calculated on the basis of geometrical acceptance.

This selection also eliminates most $e^+ e^-$ pairs from inclusive $B \rightarrow J/\psi X$ decays. Electron candidates that can be combined with an oppositely charged electron to form an invariant mass consistent with the J/ψ hypothesis, $2.90 < M_{ee} < 3.15$ GeV/c², are excluded from the tag sample if $\cos \alpha < -0.2$.

The contribution of unlike-sign pairs from the same B decay satisfying Eq. 1 is approximately 2%. After subtraction of background contributions from continuum, photon conversions and Dalitz decays, the observed opening angle distribution (without the requirement) contains a flat contribution from electron pairs from different B mesons and a contribution from electron pairs from the same B , which peaks at $\cos \alpha = -1$. The shape of the non-flat background is taken from Monte Carlo simulation and the relative normalization of the two contributions is determined by a fit to the data, which is performed separately for each 100 MeV/c-wide momentum bin below 1.2 GeV/c. The integral over the fitted non-flat contribution between the minimal allowed value of $\cos \alpha$ and 1 is taken as the residual background (Figure 2). The very small background above 1.2 GeV/c (0.8% of the total contribution) is determined from Monte Carlo simulation with a relative uncertainty of 50%.

We have studied systematic uncertainties in the predicted opening angle distributions by varying the branching fractions of $B \rightarrow D e \nu$, $B \rightarrow D^* e \nu$, $B \rightarrow D^{**} e \nu$ and non-resonant $B \rightarrow D^{(*)} \pi e \nu$ decays by one standard deviation around current average values [1]. Based on detailed studies and variations of the fit, the combined

systematic error for this background is estimated to be 5%.

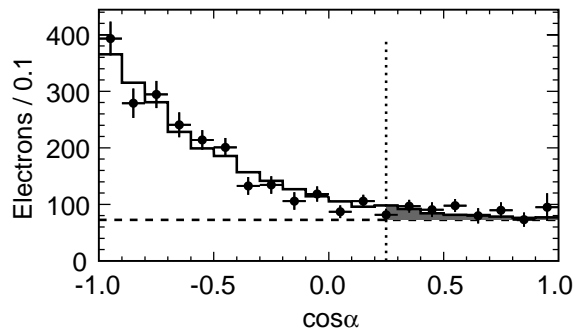


FIG. 2: Distribution of the cosine of the opening angle of unlike-sign pairs for $0.7 < p^* < 0.8 \text{ GeV}/c$. The points represent the data and the histogram is the result of a fit. The shaded area represents the estimated contribution of background electrons, and the vertical dashed line indicates the requirement on the opening angle.

Figure 3 shows the observed momentum spectra and the individual background contributions discussed so far, corrected for tracking efficiency; a summary of yields is given in Table I. Following this initial set of background corrections, the electron yield is corrected for electron identification efficiency.

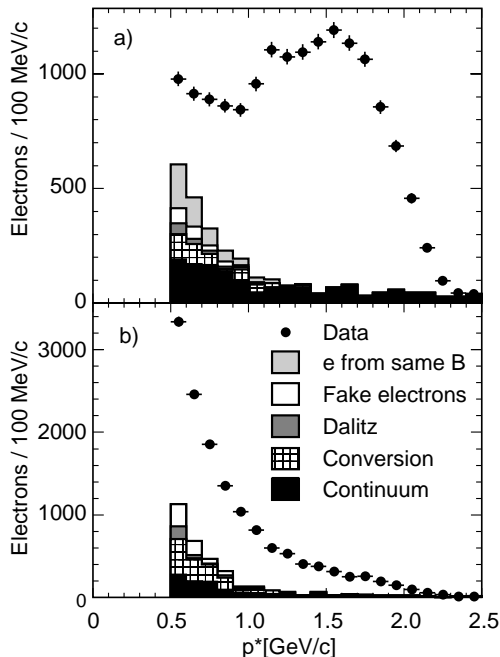


FIG. 3: Total measured spectrum (points) and estimated backgrounds (histograms) for signal electron candidates in (a) the e^+e^- sample, and (b) the $e^\pm e^\pm$ sample.

Background contributions from $B \rightarrow \bar{D}D_{(s)}X$, $D_{(s)} \rightarrow e\nu_e Y$ decays and $B \rightarrow \tau \rightarrow e$ decays are estimated by Monte Carlo simulation, using the currently known branching fractions. Combining $\mathcal{B}(D_s \rightarrow X e \nu) = (8.12 \pm 0.68)\%$, which is computed from the average D branching fraction $\mathcal{B}(D^{0,+} \rightarrow X e \nu)$ [1] and the lifetime ratios $\tau_{D^{0,+}}/\tau_{D_s}$, with $\mathcal{B}(B \rightarrow D_s X) = (9.8 \pm 3.7)\%$ [8] yields $\mathcal{B}(B \rightarrow D_s \rightarrow e) = (0.80 \pm 0.31)\%$. We take the inclusive branching fraction $\mathcal{B}(B \rightarrow \bar{D}D^{(*)}X)$ to be $(8.2 \pm 1.3)\%$ [8]. Assuming equal production rates of D and D^* , but allowing for any ratio in the systematic error, we arrive at $\mathcal{B}(B \rightarrow D \rightarrow e) = (0.84 \pm 0.21)\%$. To estimate the contribution of electrons from τ decays, we use $\mathcal{B}(B \rightarrow X \tau \nu) = (2.6 \pm 0.2)\%$, $\mathcal{B}(D_s \rightarrow \tau \nu) = (5.79 \pm 2.00)\%$ [9] and $\mathcal{B}(\tau \rightarrow e \nu_e \bar{\nu}_\tau) = (17.83 \pm 0.06)\%$ [1]. This leads to $\mathcal{B}(B \rightarrow \tau \rightarrow e) = (0.565 \pm 0.063)\%$, where the τ lepton originates either directly from a B decay or a $B \rightarrow D_s \rightarrow \tau$ cascade. The background from J/ψ and $\psi(2S)$ decays into two electrons is also estimated from Monte Carlo simulation, with $\mathcal{B}(B \rightarrow J/\psi \rightarrow e^+e^-) = (6.82 \pm 0.38) \times 10^{-4}$ and $\mathcal{B}(B \rightarrow \psi(2S) \rightarrow e^+e^-) = (3.1 \pm 0.6) \times 10^{-5}$ [1].

The tag electron sample is first corrected for continuum background and hadron misidentification. The remaining background is from secondary decays of charm particles and unvetted $J/\psi \rightarrow e^+e^-$ decays. All these contributions are estimated by Monte Carlo simulation, leading to the background-subtracted number of tag electrons $N_{\text{tag}} = 304,048 \pm 880(\text{stat}) \pm 2,100(\text{syst})$ (Table I), including a correction for signal loss due to the J/ψ -veto.

Due to $B^0\bar{B}^0$ flavor oscillations, electrons from primary B decays and $B \rightarrow \bar{D}X$, $\bar{D} \rightarrow e^- \nu_e Y$ cascades contribute to both unlike- and like-sign spectra. Denoting the efficiency of the opening angle cut as $\epsilon_\alpha(p^*)$, their p^* distributions can be written as

$$\frac{1}{\epsilon_\alpha(p^*)} \frac{dN^{+-}}{dp^*} = \frac{dN_{B \rightarrow X e \nu}}{dp^*} (1 - \chi) + \frac{dN_{B \rightarrow \bar{D} \rightarrow X e \nu}}{dp^*} \chi,$$

$$\frac{dN^{\pm\pm}}{dp^*} = \frac{dN_{B \rightarrow X e \nu}}{dp^*} \chi + \frac{dN_{B \rightarrow \bar{D} \rightarrow X e \nu}}{dp^*} (1 - \chi),$$

where χ is the product of the $B^0\bar{B}^0$ mixing parameter $\chi_0 = 0.174 \pm 0.009$ [1] and $f_0 = \mathcal{B}(\Upsilon(4S) \rightarrow B^0\bar{B}^0)$. Since the measured ratio of charged to neutral $\Upsilon(4S)$ decays is consistent with unity [10], we assume $f_0 = 0.500 \pm 0.025$, where the error is taken from [10]. We use these linear equations to determine the primary electron spectrum from B decays, $dN_{B \rightarrow X e \nu}/dp^*$. Integration of this spectrum between 0.6 and 2.5 GeV/c yields $N_{B \rightarrow X e \nu} = 25,070 \pm 410(\text{stat})$. Using Monte Carlo simulation, we determine the relative efficiency for selecting events with two electrons compared to events with a single tag to be $\epsilon_{\text{evt}} = (98.0 \pm 0.5)\%$. Together with the polar angle acceptance $\epsilon_{\text{geom}} = 84\%$, we obtain the partial branching

TABLE I: Electron yield for the three samples and corrections with statistical and systematic errors.

	(1) tag sample $1.4 < p^* < 2.3 \text{ GeV}/c$	(2) e^+e^- sample, cut on α $0.6 < p^* < 2.5 \text{ GeV}/c$	(3) $e^\pm e^\pm$ sample, all α $0.6 < p^* < 2.5 \text{ GeV}/c$
On $\Upsilon(4S)$	$395,791 \pm 630$	$14,692 \pm 120$	$10,838 \pm 110$
Continuum	$82,073 \pm 590 \pm 410$	$1,301 \pm 76 \pm 7$	$939 \pm 64 \pm 5$
$\gamma \rightarrow e^+e^-$	$561 \pm 23 \pm 140$	$283 \pm 40 \pm 37$	$856 \pm 82 \pm 110$
$\eta, \pi^0 \rightarrow \gamma e^+e^-$	$92 \pm 9 \pm 23$	$51 \pm 22 \pm 10$	$80 \pm 82 \pm 15$
Faked e	$1,455 \pm 140 \pm 360$	$136 \pm 16 \pm 20$	$348 \pm 48 \pm 52$
e from same B		$317 \pm 7 \pm 16$	
Yield before and after eff. corr.	$311,610 \pm 870 \pm 570$	$12,603 \pm 150 \pm 46$ $14,134 \pm 180 \pm 170$	$8,616 \pm 180 \pm 120$ $9,734 \pm 190 \pm 200$
$B \rightarrow \tau \rightarrow e$		$353 \pm 17 \pm 42$	$93 \pm 9 \pm 11$
$B \rightarrow D_s \rightarrow e$		$293 \pm 19 \pm 110$	$72 \pm 9 \pm 28$
$B \rightarrow D \rightarrow e$		$226 \pm 16 \pm 57$	$65 \pm 8 \pm 16$
Secondary tags	$8,073 \pm 91 \pm 2,000$	$296 \pm 17 \pm 74$	$886 \pm 29 \pm 220$
e from J/ψ or $\psi(2S)$	$1,925 \pm 42 \pm 120$	$77 \pm 8 \pm 5$	$119 \pm 10 \pm 7$
e removed by J/ψ veto	$-(2,435 \pm 50 \pm 220)$		
Net e yield	$304,048 \pm 880 \pm 2,100$	$12,890 \pm 180 \pm 230$	$8,500 \pm 200 \pm 300$

fraction

$$\mathcal{B}(B \rightarrow Xev, p^* > 0.6 \text{ GeV}/c) = \frac{N_{B \rightarrow Xev}}{N_{tag} \epsilon_{brem} \epsilon_{evt} \epsilon_{geom}}$$

$$= (10.24 \pm 0.17(\text{stat}) \pm 0.26(\text{syst}))\% ,$$

which includes a correction for the small loss of electrons due to bremsstrahlung in the detector material and the limited momentum resolution, $1 - \epsilon_{brem} = (2.20 \pm 0.35)\%$. The contributions to the systematic error are listed in Table II. Figure 4 shows the momentum spectrum of primary electrons.

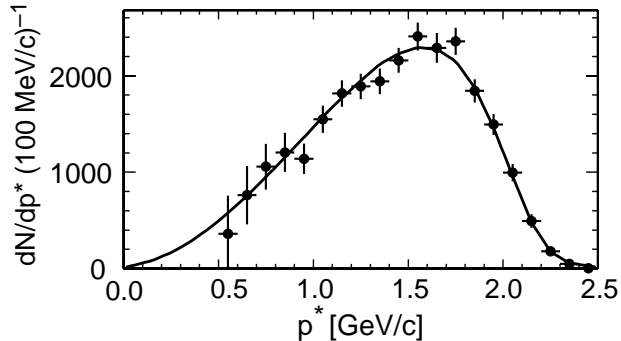


FIG. 4: Momentum spectrum of electrons from decays $B \rightarrow Xev$ after correction for efficiencies and external bremsstrahlung, with combined statistical and systematic errors. The curve indicates the fit used for the extrapolation to $p^* = 0$.

To determine the total semileptonic branching fraction, we need to extrapolate the spectrum to $p^* = 0$. This is

achieved by fitting the data to the sum of the spectra from the various exclusive decays. We use a parameterization of HQET-derived form factors [11, 12] to model the decays $B \rightarrow Dev$ and $B \rightarrow D^*ev$, and the work of Goity and Roberts [13] for non-resonant $B \rightarrow D^{(*)}\pi ev$ decays. Semileptonic B decays to $D^{**}ev$ and charmless mesons are described by the ISGW2 model [14], which is also used as an alternative description for the processes $B \rightarrow Dev$ and $B \rightarrow D^*ev$. Photon radiation in the final state is modeled by PHOTOS [15]. The relative contributions of the different exclusive decay modes are constrained to be within two standard deviations of the measured average branching fractions [1]. The best estimate for the extrapolation factor is $1 + \kappa = 1.061 \pm 0.009$, where the error accounts for the observed variations of the fit results for different decay models and branching fractions. This extrapolation leads to a total semileptonic branching fraction \mathcal{B}_{SL} of

$$\mathcal{B}(B \rightarrow Xev) = (10.87 \pm 0.18(\text{stat}) \pm 0.30(\text{syst}))\% .$$

One of the limiting factors of this analysis is the background at low momenta, especially semileptonic decays of charmed mesons produced in $b \rightarrow c\bar{c}s$ decays. As shown in Table III, raising the minimum momentum requirement p_{min}^* reduces the systematic uncertainty due to this background substantially, but also increases the error on the extrapolation to $p^* = 0$. We choose $p_{min}^* = 0.6 \text{ GeV}/c$ for the final result, since the systematic error is comparable with higher values of p_{min}^* , while the model-dependence is significantly lower.

Based on the work by Hoang *et al.* [16], we relate the

TABLE II: Impact of systematic uncertainties on \mathcal{B}_{SL} .

Source	$\Delta\mathcal{B}_{SL}(\%)$	Source	$\Delta\mathcal{B}(\%)$
e efficiency	0.144	$B \rightarrow \tau \rightarrow e$	0.044
$B \rightarrow D_s \rightarrow e$	0.130	$\gamma \rightarrow e^+e^-$	0.042
ϵ_{trk}	0.120	ϵ_{brem}	0.039
extrapolation	0.092	faked e	0.024
N_{tag}	0.075	e from same B	0.022
$B \rightarrow D \rightarrow e$	0.067	$\pi^0, \eta \rightarrow \gamma e^+e^-$	0.014
mistagged e	0.061	continuum	0.008
$f_0\chi_0$	0.059	$J/\psi, \psi(2S) \rightarrow e^+e^-$	0.003
ϵ_{evt}	0.054		
Total			0.296

TABLE III: Determination of κ , \mathcal{B}_{SL} , and the contributions to the systematic error for different signal electron momentum cut-offs. All numbers are stated in percent.

$p_{min}^*[\text{GeV}/c]$	0.5	0.6	0.7	0.8	0.9	1.0
κ	3.8	6.1	9.3	13.6	19.2	27.2
\mathcal{B}_{SL}	10.79	10.87	10.87	10.82	10.80	10.93
$\Delta\mathcal{B}_{SL}(\gamma, \pi^0)$	0.07	0.04	0.03	0.02	0.02	0.01
$\Delta\mathcal{B}_{SL}(\epsilon_{trk})$	0.12	0.12	0.12	0.12	0.12	0.12
$\Delta\mathcal{B}_{SL}(e \text{ eff.})$	0.15	0.14	0.14	0.12	0.11	0.10
$\Delta\mathcal{B}_{SL}(B \rightarrow D_s)$	0.17	0.13	0.09	0.06	0.05	0.04
$\Delta\mathcal{B}_{SL}(B \rightarrow D)$	0.10	0.07	0.05	0.03	0.02	0.01
$\Delta\mathcal{B}_{SL}(B \rightarrow \tau)$	0.05	0.04	0.04	0.03	0.03	0.02
$\Delta\mathcal{B}_{SL}(\text{extrapolation})$	0.06	0.09	0.13	0.19	0.25	0.33
$\Delta\mathcal{B}_{SL}(\text{other})$	0.15	0.14	0.14	0.15	0.15	0.17
$\Delta\mathcal{B}_{SL}(\text{syst})$	0.33	0.30	0.29	0.30	0.34	0.41
$\Delta\mathcal{B}_{SL}(\text{stat})$	0.21	0.18	0.16	0.16	0.15	0.15

decay rate and the modulus of the CKM matrix element V_{cb} by

$$|V_{cb}| = (41.9 \pm 2.0) \times 10^{-3} \times \sqrt{\mathcal{B}(B \rightarrow X_c e \nu) / 0.105} \sqrt{1.6 \text{ ps} / \tau_B}.$$

Using $\tau_B = (1.601 \pm 0.021) \text{ ps}$ and $\mathcal{B}(B \rightarrow X_u e \nu) = (1.7 \pm 0.6) \times 10^{-3}$ [1], we obtain $|V_{cb}| = 0.0423 \pm 0.0007(\text{exp}) \pm 0.0020(\text{theory})$.

In conclusion, we have used electrons in $\Upsilon(4S)$ decays tagged by a high momentum electron to measure $\mathcal{B}(B \rightarrow X e \nu) = (10.87 \pm 0.18(\text{stat}) \pm 0.30(\text{syst}))\%$. This measurement is largely model-independent. The result is in agreement with previous measurements [4, 17], but the systematic uncertainties are reduced. However, the poorly known branching fractions in B and $D_{(s)}$ decays lead to significant systematic uncertainties in the back-

ground subtraction. The resulting measurement of $|V_{cb}|$ remains dominated by theoretical uncertainties. It has recently been shown that non-perturbative effects can be assessed by measurements of moments of inclusive distributions [18].

We are grateful for the excellent luminosity and machine conditions provided by our PEP-II colleagues, and for the substantial dedicated effort from the computing organizations that support BABAR. The collaborating institutions wish to thank SLAC for its support and kind hospitality. This work is supported by DOE and NSF (USA), NSERC (Canada), IHEP (China), CEA and CNRS-IN2P3 (France), BMBF and DFG (Germany), INFN (Italy), NFR (Norway), MIST (Russia), and PPARC (United Kingdom). Individuals have received support from the A. P. Sloan Foundation, Research Corporation, and Alexander von Humboldt Foundation.

- * Also with Università di Perugia, I-06100 Perugia, Italy
- [1] D.E. Groom *et al.*, Eur. Phys. J. **C15** (2000) 1.
[2] I.I. Bigi, B. Blok, M. Shifman, A. Vainshtein, Phys. Lett. **B323** (1994) 408.
[3] H. Albrecht *et al.*, ARGUS Collaboration, Phys. Lett. **B318** (1993) 397.
[4] B. Barish *et al.*, CLEO Collaboration, Phys. Rev. Lett. **76** (1996) 1570.
[5] B. Aubert *et al.*, BABAR Collaboration, Nucl. Instrum. Meth. **A479** (2002) 1.
[6] PEP-II, SLAC-418, LBL-5379 (1993).
[7] G.C. Fox and S. Wolfram, Phys. Rev. Lett. **41** (1978) 1581.
[8] The LEP Electroweak Working Group, CERN-EP/2001-50.
[9] A. Heister *et al.*, ALEPH Collaboration, Phys. Lett. **B528** (2002) 1.
[10] J.P. Alexander *et al.*, CLEO Collaboration, Phys. Rev. Lett. **86** (2001) 2737.
[11] J. Bartelt *et al.*, CLEO Collaboration, Phys. Rev. Lett. **82** (1999) 3746.
[12] J.E. Duboscq *et al.*, CLEO Collaboration, Phys. Rev. Lett. **76** (1996) 3898.
[13] J.L. Goity and W. Roberts, Phys. Rev. **D51** (1995) 3459.
[14] D. Scora and N. Isgur, Phys. Rev. **D52** (1995) 2783.
[15] E. Barberio and Z. Was, Comput. Phys. Commun. **79**, (1994) 291.
[16] A.H. Hoang, Z. Ligeti and A. V. Manohar, Phys. Rev. Lett. **82** (1999) 277; similar expressions have been derived by I.I. Bigi, M. Shifman, and N. Uraltsev, Ann. Rev. Nucl. Part. Science **47** (1997) 591.
[17] M. Acciarri *et al.*, L3 Collaboration, Eur. Phys. J. **C13** (2000) 47; G. Abbiendi *et al.*, OPAL Collaboration, Eur. Phys. J. **C13** (2000) 225; P. Abreu *et al.*, DELPHI Collaboration, Eur. Phys. J. **C20** (2001) 455; A. Heister *et al.*, ALEPH Collaboration, Eur. Phys. J. **C22** (2002) 613.
[18] D. Cronin-Hennessy *et al.*, CLEO Collaboration, Phys.

Rev. Lett. **87** (2001) 251808.